PHYSIOME
journal.physiomeproject.org
ISSN: 2744-6204

Reproducibility of a Physiologically Based Pharmacokinetic and Pharmacodynamic (PBPK/PD) Model of Dapagliflozin

Michelle Elias[1], Mariia Myshkina[1], Nike Nemitz[1], and Matthias König[1,2*]

[1]Humboldt-Universität zu Berlin, Faculty of Life Sciences, Department of Biology, Systems Medicine of the Liver, Unter den Linden 6, 10099 Berlin, Germany
[2]University of Stuttgart, Institute of Structural Mechanics and Dynamics in Aerospace Engineering, Pfaffenwaldring 27, 70569 Stuttgart, Germany

ORIGINAL

Abstract

A computational model in the form of a whole-body physiologically based pharmacokinetic/pharmacodynamic (PBPK/PD) model of dapagliflozin was developed to systematically evaluate the influence of patient-specific factors on drug disposition. Based on curated data from 28 clinical studies, the model simulates the absorption, distribution, metabolism and excretion (ADME) of the drug as well as its pharmacodynamics. The model accounts for variability in renal and hepatic function, and effects of food intake. The model is implemented in the Systems Biology Markup Language (SBML) standard. Analysis were performed utilizing the libroadrunner simulation library. Here, we demonstrate the computational reproducibility of the key findings from the primary publication, thereby verifying the consistency of the model implementation with the published results.

Keywords: Dapagliflozin, PBPK/PD, SBML, Pharmacokinetics, Pharmacodynamics, Computational Model

Curated Model Implementation
https://doi.org/10.5281/zenodo.18011516

Primary Publications

N. Nemitz, M. Elias, and M. König. A Physiologically Based Pharmacokinetic and Pharmacodynamic (PBPK/PD) Model of Dapagliflozin in Type 2 Diabetes Mellitus: The Effect of Dosing, Hepatorenal Impairment, and Food. *Pharmaceutics*, Dec. 2025.

1 Introduction

In the primary publication (Nemitz et al., 2025), a whole-body physiologically based pharmacokinetic/pharmacodynamic (PBPK/PD) model of dapagliflozin, an sodium-glucose co-transporter 2 (SGLT2) inhibitor prescribed for the management of type 2 diabetes mellitus (T2DM), was developed to mechanistically integrate factors driving variability. The model mechanistically integrates the key factors driving variability of dapagliflozin pharmacokinetics and pharmacodynamics, such as differences in renal (Kasichayanula et al., 2011a, 2013b) and/or hepatic (Kasichayanula et al., 2011c) function, and effects of food intake (Kasichayanula et al., 2011d). The model's structure and parameters were derived from a comprehensive dataset curated from 28 published clinical studies. The dataset is available via the pharmacokinetics database PK-DB (Grzegorzewski et al., 2021) and within the model files. The model's development and scientific validation are described in detail in the primary paper (Nemitz et al., 2025).

OPEN ACCESS
Reproducible Model

***Corresponding author**
koenigmx@hu-berlin.de

Here, we present the original model, encoded in the Systems Biology Markup Language (SBML) (Hucka et al., 2019; Keating et al., 2020), and the accompanying simulation scripts required to run the simulations and reproduce the key results presented in the primary publication.

2 Model Description

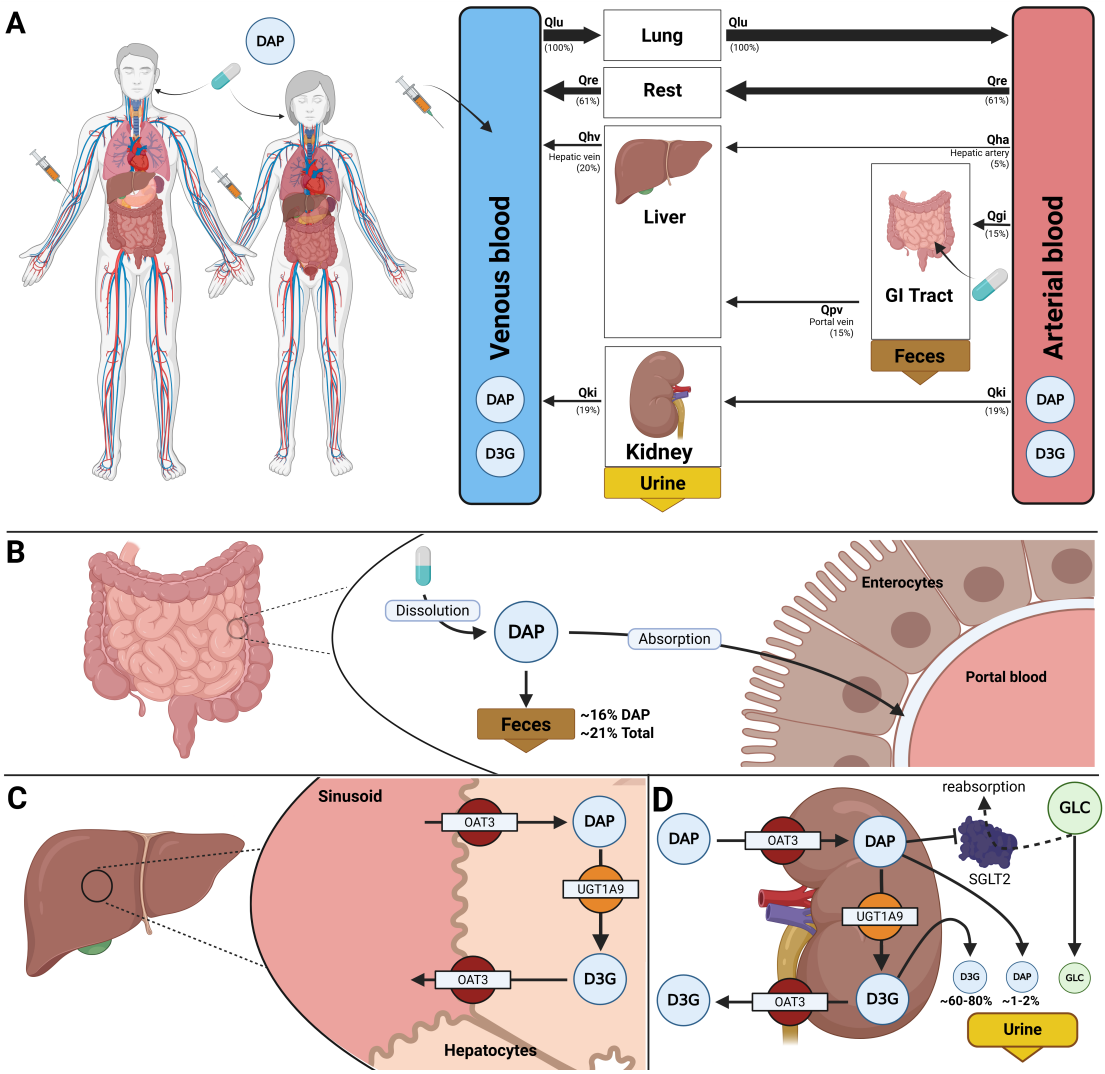

Figure 1. Whole-body PBPK/PD model of dapagliflozin and key factors influencing its disposition. A) Whole-body model illustrating dapagliflozin (DAP) administration (oral and intravenous), its systemic circulation via venous and arterial blood, and the key organs (liver, kidney, GI tract) involved in DAP metabolism, distribution, and excretion. **B)** Intestine model describing the absorption of DAP by enterocytes. DAP has a high bioavailability, with about 16% excreted in feces. **C)** Hepatic model depicting the uptake of DAP by hepatocytes and its conversion by UGT1A9 into its primary metabolite dapagliflozin-3-O-glucuronide (D3G). **D)** Renal model showing the uptake and excretion of DAP and D3G in urine and metabolic conversion of dapagliflozin to D3G. In the kidneys, dapagliflozin inhibits SGLT2, resulting in reduced glucose reabsorption and increased urinary glucose excretion.

The disposition of dapagliflozin is described using a whole-body physiologically based pharmacokinetic/pharmacodynamic (PBPK/PD) model. The model consists of interconnected compartments that simulate key organs involved in the drug's absorption, distribution, metabolism, and excretion (ADME) as well as in its pharmacodynamics. The mathematical framework of the model consists

of ordinary differential equations (ODEs). A schematic overview of the model structure is provided in Figure 1.

The model integrates the three main organ submodels, which are interconnected via systemic circulation. The gastrointestinal tract model simulates the dissolution of orally administered dapagliflozin, its subsequent first-order absorption, and its fecal excretion. The liver model describes the primary metabolic pathway, where dapagliflozin is converted to its major metabolite dapagliflozin-3-O-glucuronide (D3G). The kidney model implements the renal excretion of dapagliflozin, D3G, and glucose, as well as the conversion of dapagliflozin to D3G. The pharmacodynamic component links dapagliflozin concentration in the kidneys to urinary glucose excretion (UGE) through inhibition of renal glucose reabsorption. This process is affected by fasting plasma glucose and the renal threshold for glucose.

The model accounts for patient-specific factors through the corresponding scaling parameters. Renal impairment was modeled as a progressive decline in renal function by scaling the factor f_{renal}. Hepatic impairment was modeled as a gradual increase in cirrhosis by scaling liver function with the parameter $f_{cirrhosis}$. Food effect was incorporated via the intestinal absorption scaling factor $f_{absorption}$.

The PBPK/PD model and its tissue-specific submodels were developed using the Systems Biology Markup Language (SBML) (Hucka et al., 2019; Keating et al., 2020). Programming and visualization of the models were performed using the `sbmlutils` (König, 2024) and `cy3sbml` (König et al., 2012) libraries. Numerical solutions for the ordinary differential equations (ODEs) underlying the model were computed using `sbmlsim` (König, 2021), which is powered by the high-performance SBML simulation engine `libroadrunner` (Welsh et al., 2023; Somogyi et al., 2015). The tissue submodels were developed as SBML submodels and coupled with the whole-body model using the hierarchical model composition (comp) SBML extension (Smith et al., 2015). The complete model, submodels, reference simulations, and visualizations are available as a COMBINE archive (OMEX) (Bergmann et al., 2014, 2015). The model is annotated with extensive metadata using the open modeling and exchange (OMEX) metadata specification (Neal et al., 2020, 2019). The model was validated using the SBML validator, with the model passing all validation tests without errors or warnings. The FAIRness of the model was increased by following the FAIRification of computational models in the biological workflow (Balaur et al., 2025).

The model and all associated materials (mathematical formulation, simulation scripts, parameters, and documentation) are publicly available in SBML format and OMEX archive under a CC-BY 4.0 license at https://github.com/matthiaskoenig/dapagliflozin-model, with version 0.9.8 Nemitz et al. (2025) used in the publication and for model validation.

3 Computational Simulation

All simulations were performed using `Python 3.13` together with the high-performance `libRoadRunner` simulation engine. The workflow was tested across multiple platforms, including Ubuntu 24.04/25.10 and Windows 11. For SBML model handling and simulation, we relied on the `sbmlutils` and `sbmlsim` libraries, while data management and figure generation were carried out with standard scientific Python packages.

To ensure reproducibility, we provide two equivalent setups for regenerating all figures presented in Section 4: (1) a local Python installation using `uv`, and (2) a containerized workflow using Docker. Both approaches reproduce all results from the primary publication. Reproducibility is continuously validated through automated integration tests, with results available at https://github.com/matthiaskoenig/dapagliflozin-model/actions.

3.1 Python with uv (local install)

This workflow installs the package directly on your machine using `uv`.

Prerequisite: `uv` must be installed on your system (https://docs.astral.sh/uv/getting-started/installation/).

Clone the repository and move into its folder:

```
git clone https://github.com/matthiaskoenig/dapagliflozin-model.git
cd dapagliflozin-model
git checkout 0.9.8
```

Set up the uv virtual environment and install all dependencies:

```
uv sync
```

Run the complete analysis:

```
uv run run_dapagliflozin -a all -r results
```

All reproduced figures and outputs are written to `./results/` inside the repository.

Alternatively, you can use any other way to setup a local python environment (e.g. conda) and install the package after cloning the repository via:

```
pip install -e .
```

or directly from the main branch via:

```
pip install git+https://github.com/matthiaskoenig/dapagliflozin-model.git@0
    .9.8
```

The full analysis can be run in the python environment via:

```
(env) run_dapagliflozin -a all -r results
```

3.2 Docker (containerized)

This workflow runs the analysis in a preconfigured Docker container.

Prerequisite: Docker must be installed on your system (https://docs.docker.com/get-docker/).

Start the container and mount a local `results/` directory:

```
docker run -v "${PWD}/results:/results" -it matthiaskoenig/dapagliflozin
    :0.9.8 /bin/bash
```

Inside the container, run the analysis. Results will be written to the mounted folder:

```
uv run run_dapagliflozin -a all -r /results
```

The reproduced figures and outputs are then accessible on the host system in `./results/`.

If file access is restricted on Linux due to permissions, adjust ownership and rights as follows:

```
sudo chown $(id -u):$(id -g) -R "${PWD}/results"
sudo chmod 775 "${PWD}/results"
```

3.3 Available Options

Specific parts of the analysis can be executed by providing command-line arguments. A full overview of the available options is obtained via:

```
uv run run_dapagliflozin --help
```

3.4 Outputs

The workflow reproduces all figures and results from the primary publication, including:

- Study simulations (Figures 2–3)
- Simulation experiments and scans (Figures 5–6)

All results are stored in the `results/` directory. This directory contains the individual figure panels in PNG format as well as an automatically generated HTML report (`index.html`) that consolidates all figures into a single document. The content of this report directly corresponds to Figures 2–6 in the manuscript.

4 Reproducibility Goals

The reproducibility of the dapagliflozin PBPK/PD model was confirmed by reproducing key figures from the original publication and its supplementary material. The figures presented here are a selection chosen to demonstrate consistent reproduction of results across different dose levels, pathophysiological, and prandial states. Tables 1–2 provide an overview of the simulation observables and the parameter changes specific to each study, experiment, or scan. The model and simulation scripts can be used to reproduce the full set of results from the original study and its supplements.

Table 1. Plotted observables and parameter changes per study simulation. Square brackets around SBML species ids indicate concentrations (amount/volume units). Square brackets enclosing numerical values indicate parameter ranges, whereas curly brackets indicate sets of discrete choices.

StudyID	Plotted	Changes
Boulton2013 (Boulton et al., 2013)	`[Cve_dap]`	`PODOSE_dap = 10 mg` `IVDOSE_dap = 80 µg`
Cho2021 (Cho et al., 2021)	`[Cve_dap]`	`BW = 72.8 kg` `PODOSE_dap = 10 mg`
FDAMB102002 (FDA, 2013a)	`[Cve_dap]`, `KI__UGE`	`PODOSE_dap` $\in \{2.5, 10, 20, 50, 100\}$ mg
FDAMB102003 (FDA, 2013b)	`[Cve_dap]`, `Aurine_dap`, `KI__UGE`	`PODOSE_dap` $\in \{5, 25, 100\}$ mg `KI__glc_ext = 7.5 (T2DM)`
FDAMB102006 (FDA, 2013c)	`Aurine_daptot`, `Aurine_dap`, `Aurine_d3g`, `Afeces_daptot`, `Afeces_dap`	`PODOSE_dap = 50 mg`
FDAMB102007 (FDA, 2013d)	`Aurine_dap`, `Aurine_d3g`, `KI__UGE`	`PODOSE_dap` $\in \{20, 50\}$ mg `KI__glc_ext = 7.5 (T2DM)` `f_renal_function` $\in \{0.69, 0.32, 0.19\}$
Gould2013 (Gould et al., 2013)	`KI__UGE`	`PODOSE_dap` $\in \{0, 0.001, 0.01, 0.1, 0.3, 1, 2.5, 5, 10, 20, 50, 100, 250, 500\}$ mg
Hwang2022a (Hwang et al., 2022)	`[Cve_dap]`	`PODOSE_dap = 10 mg` `BW` $\in \{67.05, 68.09, 71, 71.03, 71.13, 71.18, 71.43, 71.79, 72.44, 72.78, 73.44, 73.61\}$ kg
Imamura2013 (Imamura et al., 2013)	`[Cve_dap]`	`PODOSE_dap = 10 mg` `KI__glc_ext = 9 mM (T2DM)`
Jang2020 (Jang et al., 2020)	`[Cve_dap]`	`PODOSE_dap = 10 mg` `BW = 71.45 kg`
Kasichayanula2011 (Kasichayanula et al., 2011c)	`[Cve_dap]`, `[Cve_d3g]`	`PODOSE_dap = 10 mg` `f_cirrhosis` $\in \{0.399, 0.698, 0.813\}$ `BW` $\in \{80.9, 81.8, 87.5, 89.2\}$ kg `f_renal_function` $\in \{1.278, 1.38, 1.428, 1.583\}$

Table 1. Plotted observables and parameter changes per study simulation (continued). Square brackets around SBML species ids indicate concentrations (amount/volume units). Square brackets enclosing numerical values indicate parameter ranges, whereas curly brackets indicate sets of discrete choices.

StudyID	Plotted (sid)	Changes
Kasichayanula2011a (Kasichayanula et al., 2011a)	[Cve_dap], [Cve_d3g], KI__UGE	PODOSE_dap ∈ {0, 2.5, 10, 20} mg KI__glc_ext = 7.5 (T2DM) BW ∈ {60.2, 60.8, 61.0, 67.4} kg f_renal_function ∈ [0.88, 0.95]
Kasichayanula2011b (Kasichayanula et al., 2011d)	[Cve_dap], [Cve_d3g]	PODOSE_dap = 10 mg GU__f_absorption ∈ {1.0, 0.3}
Kasichayanula2011c (Kasichayanula et al., 2011b)	[Cve_dap]	PODOSE_dap ∈ {20, 50} mg
Kasichayanula2012 (Kasichayanula et al., 2012)	[Cve_dap]	PODOSE_dap = 20 mg
Kasichayanula2013 (Kasichayanula et al., 2013b)	[Cve_dap], [Cve_d3g], Aurine_dap, Aurine_d3g	PODOSE_dap ∈ {20, 50} mg f_renal_function ∈ {0.243, 0.426, 0.696, 1.185, 1.332} KI__glc_ext ∈ {4.94, 6.79, 7.23, 7.75, 9.32} mM BW ∈ {73.9, 77.4, 77.9, 78.4, 79.2} kg
Kasichayanula2013a (Kasichayanula et al., 2013a)	[Cve_dap], [Cve_d3g], Aurine_dap, Aurine_d3g	PODOSE_dap = 10 mg
Khomitskaya2018 (Khomitskaya et al., 2018)	[Cve_dap]	PODOSE_dap = 10 mg GU__f_absorption = 0.3 BW = 71.9 kg
Kim2023 (Kim et al., 2023a)	[Cve_dap], KI__UGE	PODOSE_dap = 10 mg BW = 69.1 kg
Kim2023a (Kim et al., 2023b)	[Cve_dap]	PODOSE_dap = 10 mg BW = 71.5 kg KI__glc_ext = 5.3 mM
Komoroski2009 (Komoroski et al., 2009)	[Cve_dap], Aurine_dap, KI__UGE	PODOSE_dap ∈ {0, 2.5, 5, 10, 20, 50, 100, 250, 500} mg GU__f_absorption ∈ {1.0, 0.3} BW = 79 kg
LaCreta2016 (LaCreta et al., 2016)	[Cve_dap]	PODOSE_dap ∈ {2.5, 10} mg BW ∈ {70.1, 73.5} kg GU__f_absorption ∈ {1.0, 0.3}
Obermeier2010 (Obermeier et al., 2010)	[Cve_dap], [Cve_daptot]	PODOSE_dap = 50 mg
Sha2015 (Sha et al., 2015)	[Cve_dap], KI__UGE, KI__RTG	PODOSE_dap = 10 mg BW = 78.9 kg f_renal_function = 0.97
Shah2019a (Shah et al., 2019)	[Cve_dap]	PODOSE_dap = 5 mg BW = 68.4 kg GU__f_absorption ∈ {1.0, 0.3}
vanderAartvanderBeek2020 (van der Aart-van der Beek et al., 2020)	[Cve_dap]	PODOSE_dap = 10 mg
Watada2019 (Watada et al., 2019)	[Cve_dap], [Cve_d3g], KI__UGE	PODOSE_dap ∈ {0, 5, 10} mg BW ∈ {57.2, 59.8, 61.6} kg KI__glc_ext ∈ {7.41, 7.45, 7.94} mM (T1DM) f_renal_function ∈ {0.916, 0.946, 0.954}

Table 1. Plotted observables and parameter changes per study simulation (continued). Square brackets around SBML species ids indicate concentrations (amount/volume units). Square brackets enclosing numerical values indicate parameter ranges, whereas curly brackets indicate sets of discrete choices.

StudyID	Plotted (sid)	Changes
Yang2013 (Yang et al., 2013)	[Cve_dap], [Cve_d3g], KI__UGE	PODOSE_dap ∈ {5, 10} mg BW ∈ {62.2, 62.8} kg

Table 2. Plotted observables and parameter changes per simulation experiment and scan. Square brackets around SBML species ids indicate concentrations (amount/volume units). Square brackets enclosing numerical values indicate parameter ranges, whereas curly brackets indicate sets of discrete choices.

Simulation	Plotted	Changes
DoseDependencyExperiment	[Cve_dap], [Cve_d3g], Aurine_dap, Aurine_d3g, Afeces_dap, KI__RTG, KI__UGE	PODOSE_dap ∈ [0, 500] mg KI__glc_ext ∈ [3, 15] mM at fixed PODOSE_dap = 10 mg
FoodEffect	[Cve_dap], [Cve_d3g], Aurine_dap, Aurine_d3g, Afeces_dap, KI__RTG, KI__UGE	PODOSE_dap = 10 mg GU__f_absorption ∈ [0.1, 10]
HepaticRenalImpairment	[Cve_dap], [Cve_d3g], Aurine_dap, Aurine_d3g, Afeces_dap, KI__RTG, KI__UGE	PODOSE_dap = 10 mg f_cirrhosis ∈ [0.0, 0.81] KI__f_renal_function ∈ [0.19, 1.0]
DapagliflozinParameterScan	[Cve_dap], [Cve_d3g], Aurine_dap, Aurine_d3g, Afeces_dap, KI__UGE, AUC_{inf}, C_{max}, t_{half}, UGE(24 hr)	f_cirrhosis ∈ [0.0, 0.9] (PODOSE_dap = 10 mg) KI__f_renal_function ∈ [0.1, 10] (PODOSE_dap ∈ {20, 50} mg) GU__f_absorption ∈ [0.1, 10] (PODOSE_dap = 10 mg) PODOSE_dap ∈ [0.001, 500] mg KI__glc_ext ∈ [3, 15] mM

4.1 Reproduction of Study Simulations

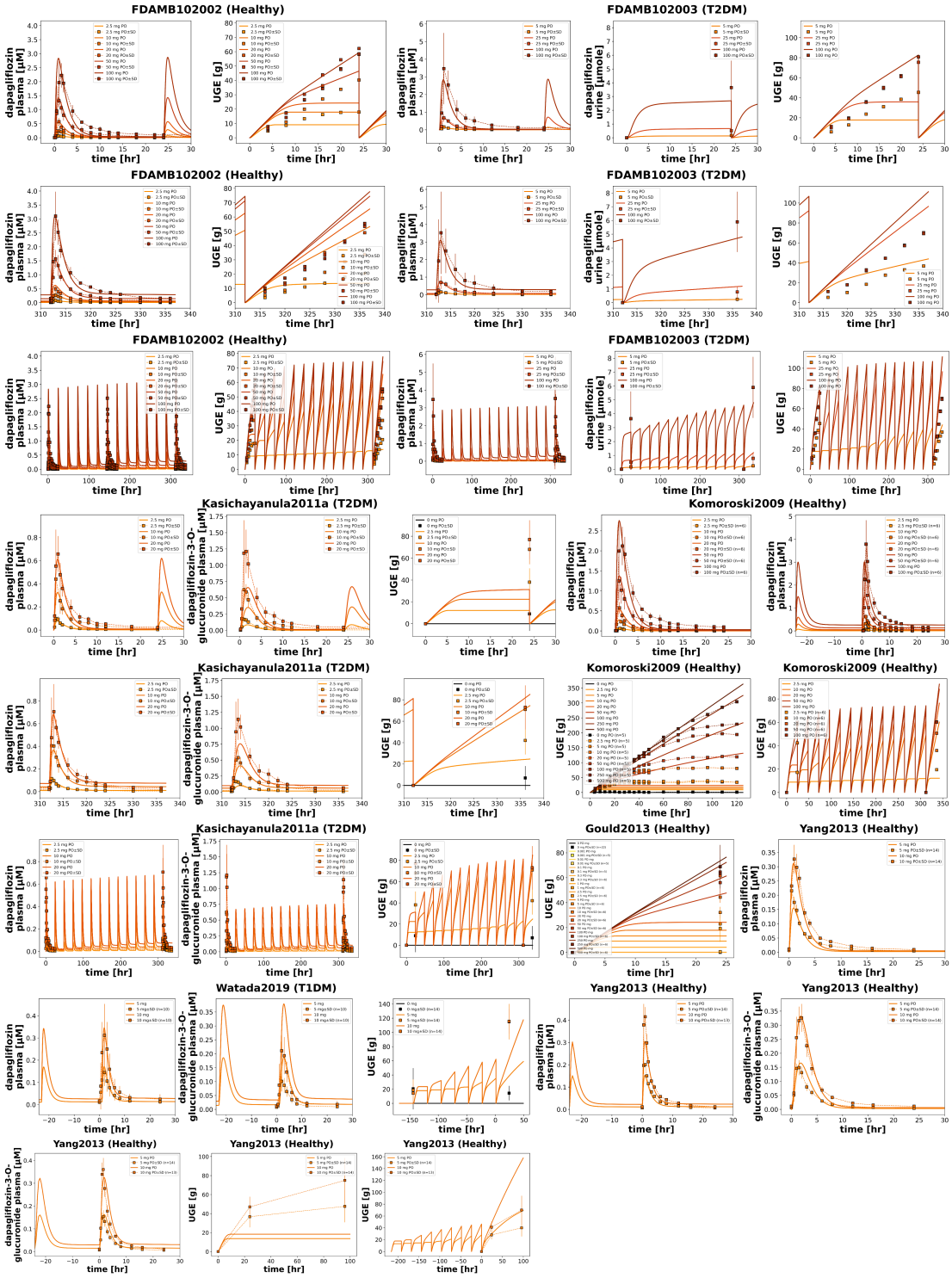

Figure 2. Reproduction of study simulations (dose dependency) from the primary publication. Data is taken from FDA (2013a,b); Gould et al. (2013); Kasichayanula et al. (2011a); Komoroski et al. (2009); Watada et al. (2019); Yang et al. (2013).

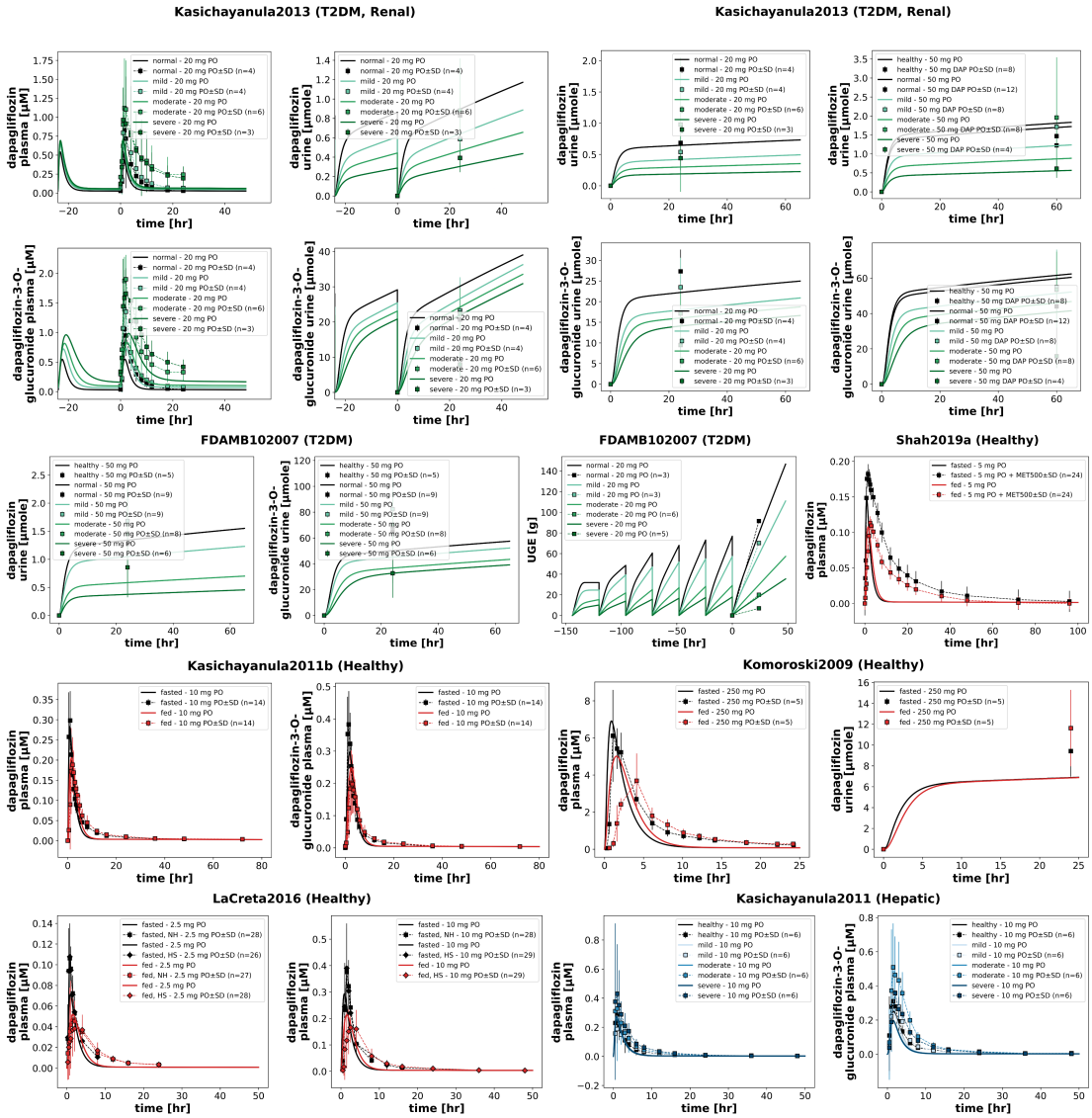

Figure 3. Reproduction of study simulations (renal impairment, hepatic impairment, and food effects) from the primary publication. Data is taken from FDA (2013d); Kasichayanula et al. (2011c,d, 2013b); Komoroski et al. (2009); LaCreta et al. (2016); Shah et al. (2019).

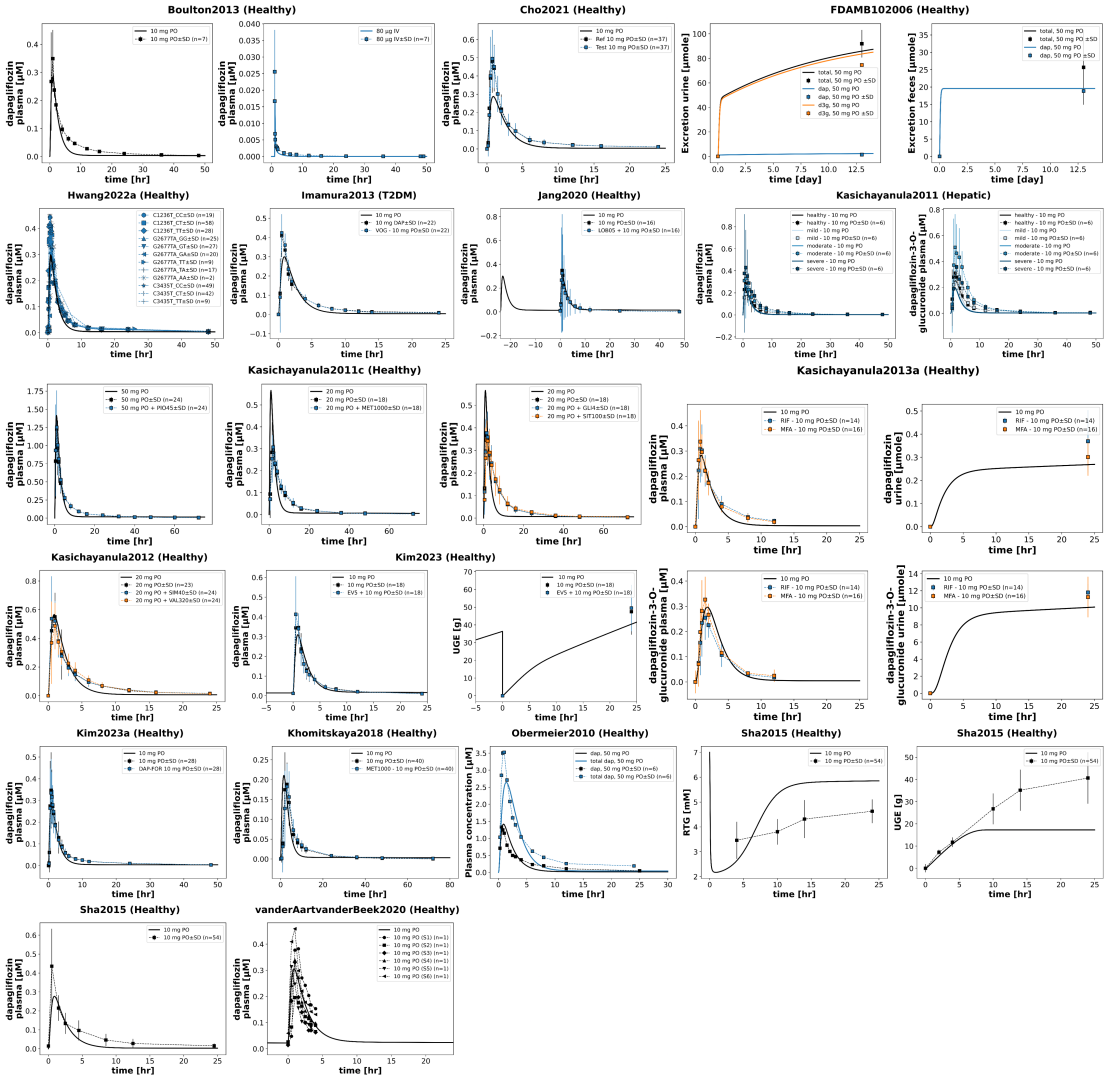

Figure 4. Reproduction of supplementary study simulations from the primary publication. Data is taken from Boulton et al. (2013); Cho et al. (2021); FDA (2013c); Hwang et al. (2022); Imamura et al. (2013); Jang et al. (2020); Kasichayanula et al. (2011c,b, 2012, 2013a); Khomitskaya et al. (2018); Kim et al. (2023a,b); Obermeier et al. (2010); Sha et al. (2015); van der Aart-van der Beek et al. (2020).

4.2 Reproduction of Simulations Experiments and Scans

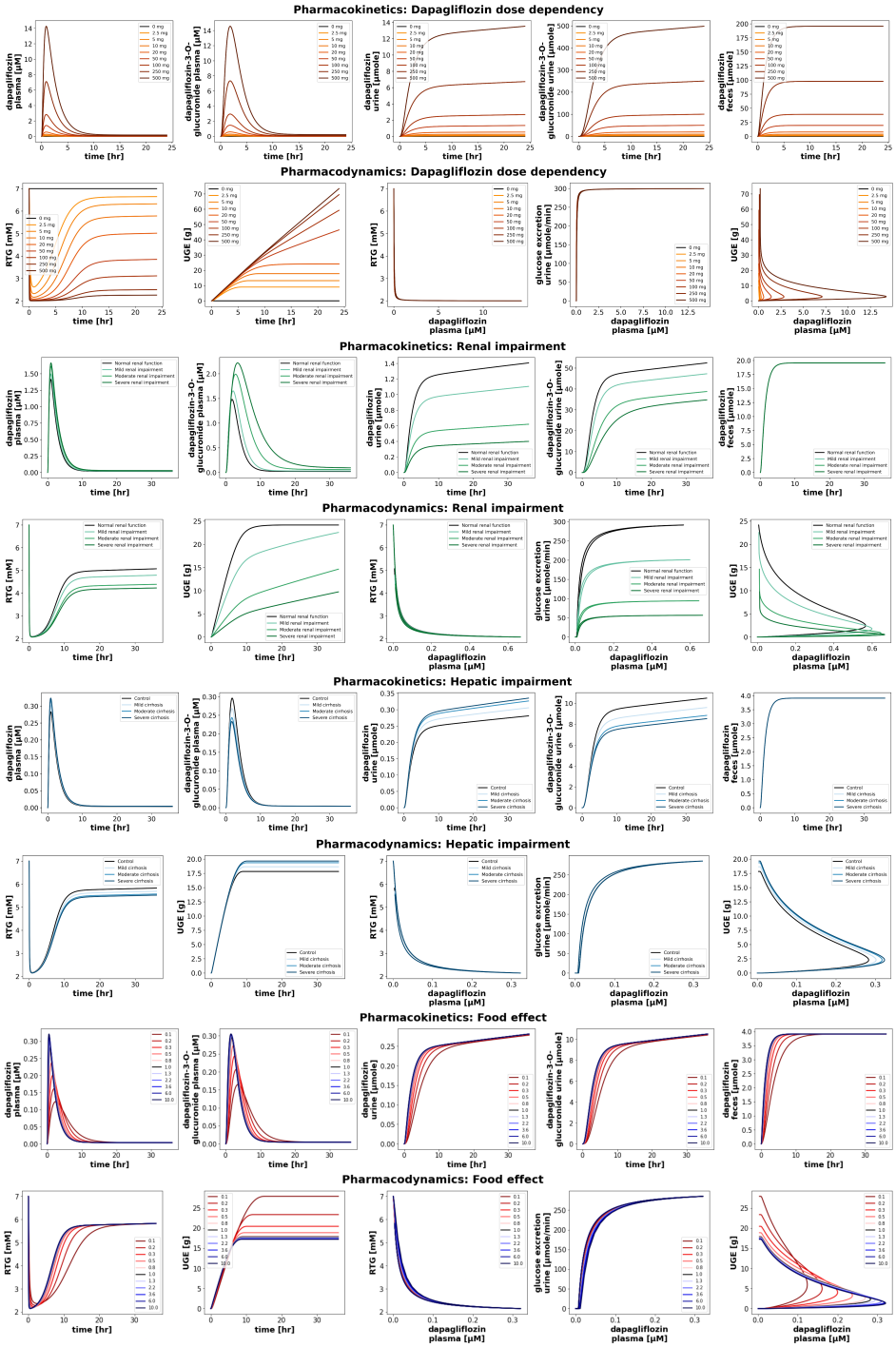

Figure 5. Reproduction of simulation experiments from the primary publication.

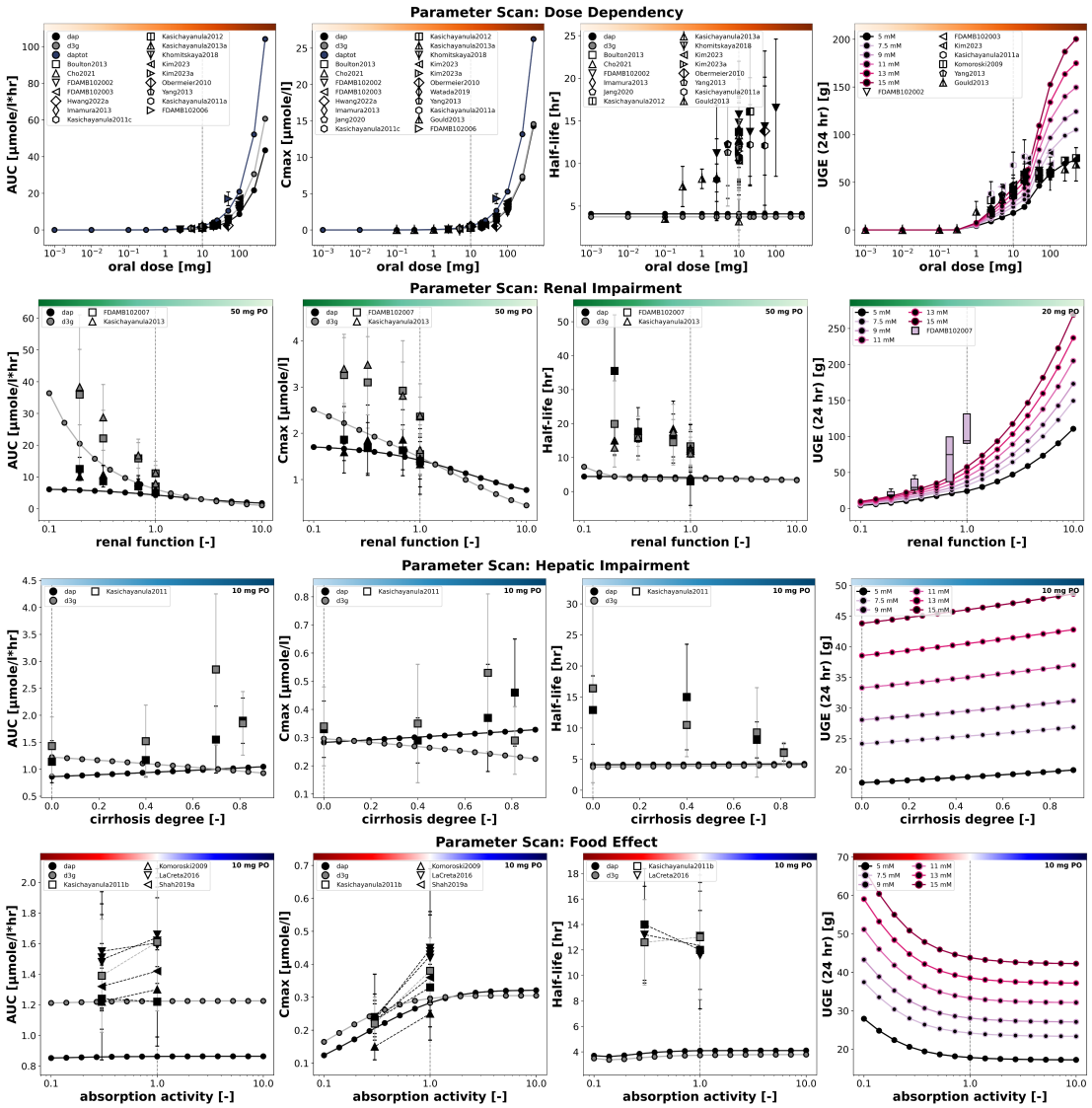

Figure 6. Reproduction of parameter scans from the primary publication. Data is taken from Boulton et al. (2013); Cho et al. (2021); FDA (2013a,b,c,d); Gould et al. (2013); Hwang et al. (2022); Imamura et al. (2013); Jang et al. (2020); Kasichayanula et al. (2011c,a,d,b, 2012, 2013b,a); Khomitskaya et al. (2018); Kim et al. (2023a,b); Komoroski et al. (2009); LaCreta et al. (2016); Obermeier et al. (2010); Shah et al. (2019); Yang et al. (2013).

5 Discussion

We have demonstrated the computational reproducibility of the key findings from the dapagliflozin PBPK/PD model presented in the primary publication. Using the provided simulation scripts, all figures were regenerated without modifying parameters or structure, verifying the consistency of the model. Reproducibility was confirmed across different operating systems using both a local installation with uv and a Dockerized workflow. The uv-based approach allows users to install the package and dependencies natively, while the containerized workflow provides a fully preconfigured environment and ensures consistent results independent of the local setup. Encoding the model in SBML with hierarchical composition removes ambiguity and allows modular reuse of the tissue submodels. Together with the use of community standards and FAIR practices, this provides a transparent and reusable resource that can be applied or extended in future pharmacokinetic/pharmacodynamic modeling work.

Author Contributions

M.E., N.N. and M.K. contributed to conceptualization, methodology, data curation, and development of the PBPK/PD model. M.E., N.N., M.M., and M.K. contributed to analyses, software, and visualization. M.E. M.M., and M.K. contributed to the reproducibility of the computational workflow. M.E. wrote the original draft. M.E., N.N., M.M., and M.K. contributed to manuscript review and editing. M.K. provided supervision throughout the project. All authors approved the final manuscript.

Funding

Matthias König (MK) was supported by the Federal Ministry of Research, Technology and Space (BMFTR, Germany) within ATLAS by grant number 031L0304B and by the German Research Foundation (DFG) within the Research Unit Program FOR 5151 "QuaLiPerF (Quantifying Liver Perfusion-Function Relationship in Complex Resection - A Systems Medicine Approach)" by grant number 436883643 and by grant number 465194077 (Priority Programme SPP 2311, Subproject SimLivA). Mariia Myshkina was supported by the Federal Ministry of Research, Technology and Space (BMFTR, Germany) within ATLAS by grant number 031L0304B and by the German Research Foundation (DFG) within the Priority Programme SPP 2311, Subproject SimLivA by grant number 465194077. This work was supported by the BMFTR-funded de.NBI Cloud within the German Network for Bioinformatics Infrastructure (de.NBI) (031A537B, 031A533A, 031A538A, 031A533B, 031A535A, 031A537C, 031A534A, 031A532B).

Acknowledgments

Figures were created in BioRender. König, M. (2025) https://BioRender.com/07h7x81.

References

I. Balaur, D. P. Nickerson, D. Welter, J. A. Wodke, F. Ancien, T. Gebhardt, V. Grouès, H. Hermjakob, M. König, N. Radde, A. Rougny, R. Schneider, R. S. Malik-Sheriff, K. B. Shiferaw, M. Stefan, V. Satagopam, and D. Waltemath. FAIRification of computational models in biology, Mar. 2025.

F. T. Bergmann, R. Adams, S. Moodie, J. Cooper, M. Glont, M. Golebiewski, M. Hucka, C. Laibe, A. K. Miller, D. P. Nickerson, B. G. Olivier, N. Rodriguez, H. M. Sauro, M. Scharm, S. Soiland-Reyes, D. Waltemath, F. Yvon, and N. Le Novère. COMBINE archive and OMEX format: One file to share all information to reproduce a modeling project. *BMC bioinformatics*, 15(1):369, Dec. 2014. ISSN 1471-2105. doi: 10.1186/s12859-014-0369-z.

F. T. Bergmann, N. Rodriguez, and N. Le Novère. COMBINE Archive Specification Version 1. *Journal of Integrative Bioinformatics*, 12(2):261, Sept. 2015. ISSN 1613-4516. doi: 10.2390/biecoll-jib-2015-261.

D. W. Boulton, S. Kasichayanula, C. F. A. Keung, M. E. Arnold, L. J. Christopher, X. S. Xu, and F. Lacreta. Simultaneous oral therapeutic and intravenous ^{14}C-microdoses to determine the absolute oral bioavailability of saxagliptin and dapagliflozin. *British journal of clinical pharmacology*, 75(3): 763–768, Mar. 2013. ISSN 1365-2125 0306-5251. doi: 10.1111/j.1365-2125.2012.04391.x.

S. Cho, J. Lee, Y. Yoo, M. Cho, S. Sohn, and B.-J. Lee. Improved Manufacturability and In Vivo Comparative Pharmacokinetics of Dapagliflozin Cocrystals in Beagle Dogs and Human Volunteers. *Pharmaceutics*, 13(1), Jan. 2021. ISSN 1999-4923. doi: 10.3390/pharmaceutics13010070.

FDA. FDA 202293Orig1s000 Review (FDAMB102002). Pharmacokinetics for multiple-dose administration of dapagliflozin in healthy subjects., Nov. 2013a.

FDA. FDA 202293Orig1s000 Review (FDAMB102003). Bioequivalence assessment during multiple-dose administration of dapagliflozin in subjects with T2DM., Nov. 2013b.

FDA. FDA 202293Orig1s000 Review (FDAMB102006). Urinary and fecal excretion data following a 50 mg dose of dapagliflozin., Nov. 2013c.

FDA. FDA 202293Orig1s000 Review (FDAMB102007). Impact of renal impairment on the pharmacokinetics and pharmacodynamics of dapagliflozin was studied in a single (50 mg) and multiple dose (20 mg)., Nov. 2013d.

J. C. Gould, S. Kasichayanula, D. C. Shepperly, and D. W. Boulton. Use of low-dose clinical pharmacodynamic and pharmacokinetic data to establish an occupational exposure limit for dapagliflozin, a potent inhibitor of the renal sodium glucose co-transporter 2. *Regulatory toxicology and pharmacology : RTP*, 67(1):89–97, Oct. 2013. ISSN 1096-0295 0273-2300. doi: 10.1016/j.yrtph.2013.07.002.

J. Grzegorzewski, J. Brandhorst, K. Green, D. Eleftheriadou, Y. Duport, F. Barthorscht, A. Köller, D. Y. J. Ke, S. De Angelis, and M. König. PK-DB: Pharmacokinetics database for individualized and stratified computational modeling. *Nucleic Acids Research*, 49(D1):D1358–D1364, Jan. 2021. ISSN 1362-4962. doi: 10.1093/nar/gkaa990.

M. Hucka, F. T. Bergmann, C. Chaouiya, A. Dräger, S. Hoops, S. M. Keating, M. König, N. L. Novère, C. J. Myers, B. G. Olivier, S. Sahle, J. C. Schaff, R. Sheriff, L. P. Smith, D. Waltemath, D. J. Wilkinson, and F. Zhang. The Systems Biology Markup Language (SBML): Language Specification for Level 3 Version 2 Core Release 2. *Journal of Integrative Bioinformatics*, 16(2), June 2019. ISSN 1613-4516. doi: 10.1515/jib-2019-0021.

J. G. Hwang, S. I. Jeong, Y. K. Kim, Y. Lee, S. C. Ji, S. Lee, and M. K. Park. Common ABCB1 SNP, C3435T could affect systemic exposure of dapagliflozin in healthy subject. *Translational and clinical pharmacology*, 30(4):212–225, Dec. 2022. ISSN 2289-0882 2383-5427. doi: 10.12793/tcp.2022.30.e23.

A. Imamura, M. Kusunoki, S. Ueda, N. Hayashi, and Y. Imai. Impact of voglibose on the pharmacokinetics of dapagliflozin in Japanese patients with type 2 diabetes. *Diabetes therapy : research, treatment and education of diabetes and related disorders*, 4(1):41–49, June 2013. ISSN 1869-6953 1869-6961. doi: 10.1007/s13300-012-0016-5.

K. Jang, J.-Y. Jeon, S. J. Moon, and M.-G. Kim. Evaluation of the Pharmacokinetic Interaction Between Lobeglitazone and Dapagliflozin at Steady State. *Clinical therapeutics*, 42(2):295–304, Feb. 2020. ISSN 1879-114X 0149-2918. doi: 10.1016/j.clinthera.2020.01.003.

S. Kasichayanula, M. Chang, M. Hasegawa, X. Liu, N. Yamahira, F. P. LaCreta, Y. Imai, and D. W. Boulton. Pharmacokinetics and pharmacodynamics of dapagliflozin, a novel selective inhibitor of sodium-glucose co-transporter type 2, in Japanese subjects without and with type 2 diabetes mellitus. *Diabetes, obesity & metabolism*, 13(4):357–365, Apr. 2011a. ISSN 1463-1326 1462-8902. doi: 10.1111/j.1463-1326.2011.01359.x.

S. Kasichayanula, X. Liu, W. C. Shyu, W. Zhang, M. Pfister, S. C. Griffen, T. Li, F. P. LaCreta, and D. W. Boulton. Lack of pharmacokinetic interaction between dapagliflozin, a novel sodium-glucose transporter 2 inhibitor, and metformin, pioglitazone, glimepiride or sitagliptin in healthy subjects. *Diabetes, obesity & metabolism*, 13(1):47–54, Jan. 2011b. ISSN 1463-1326 1462-8902. doi: 10.1111/j.1463-1326.2010.01314.x.

S. Kasichayanula, X. Liu, W. Zhang, M. Pfister, F. P. LaCreta, and D. W. Boulton. Influence of hepatic impairment on the pharmacokinetics and safety profile of dapagliflozin: An open-label, parallel-group, single-dose study. *Clinical therapeutics*, 33(11):1798–1808, Nov. 2011c. ISSN 1879-114X 0149-2918. doi: 10.1016/j.clinthera.2011.09.011.

S. Kasichayanula, X. Liu, W. Zhang, M. Pfister, S. B. Reele, A.-F. Aubry, F. P. LaCreta, and D. W. Boulton. Effect of a high-fat meal on the pharmacokinetics of dapagliflozin, a selective SGLT2 inhibitor, in healthy subjects. *Diabetes, obesity & metabolism*, 13(8):770–773, Aug. 2011d. ISSN 1463-1326 1462-8902. doi: 10.1111/j.1463-1326.2011.01397.x.

S. Kasichayanula, M. Chang, X. Liu, W.-C. Shyu, S. C. Griffen, F. P. LaCreta, and D. W. Boulton. Lack of pharmacokinetic interactions between dapagliflozin and simvastatin, valsartan, warfarin, or digoxin. *Advances in therapy*, 29(2):163–177, Feb. 2012. ISSN 1865-8652 0741-238X. doi: 10.1007/s12325-011-0098-x.

S. Kasichayanula, X. Liu, S. C. Griffen, F. P. Lacreta, and D. W. Boulton. Effects of rifampin and mefenamic acid on the pharmacokinetics and pharmacodynamics of dapagliflozin. *Diabetes, obesity & metabolism*, 15(3):280–283, Mar. 2013a. ISSN 1463-1326 1462-8902. doi: 10.1111/dom.12024.

S. Kasichayanula, X. Liu, M. Pe Benito, M. Yao, M. Pfister, F. P. LaCreta, W. G. Humphreys, and D. W. Boulton. The influence of kidney function on dapagliflozin exposure, metabolism and pharmacodynamics in healthy subjects and in patients with type 2 diabetes mellitus. *British journal of clinical pharmacology*, 76(3):432–444, Sept. 2013b. ISSN 1365-2125 0306-5251. doi: 10.1111/bcp.12056.

S. M. Keating, D. Waltemath, M. König, F. Zhang, A. Dräger, C. Chaouiya, F. T. Bergmann, A. Finney, C. S. Gillespie, T. Helikar, S. Hoops, R. S. Malik-Sheriff, S. L. Moodie, I. I. Moraru, C. J. Myers, A. Naldi, B. G. Olivier, S. Sahle, J. C. Schaff, L. P. Smith, M. J. Swat, D. Thieffry, L. Watanabe, D. J. Wilkinson, M. L. Blinov, K. Begley, J. R. Faeder, H. F. Gómez, T. M. Hamm, Y. Inagaki, W. Liebermeister, A. L. Lister, D. Lucio, E. Mjolsness, C. J. Proctor, K. Raman, N. Rodriguez, C. A. Shaffer, B. E. Shapiro, J. Stelling, N. Swainston, N. Tanimura, J. Wagner, M. Meier-Schellersheim, H. M. Sauro, B. Palsson, H. Bolouri, H. Kitano, A. Funahashi, H. Hermjakob, J. C. Doyle, M. Hucka, and SBML Level 3 Community members. SBML Level 3: An extensible format for the exchange and reuse of biological models. *Molecular Systems Biology*, 16(8):e9110, Aug. 2020. ISSN 1744-4292. doi: 10.15252/msb.20199110.

Y. Khomitskaya, N. Tikhonova, K. Gudkov, S. Erofeeva, V. Holmes, B. Dayton, N. Davies, D. W. Boulton, and W. Tang. Bioequivalence of Dapagliflozin/Metformin Extended-release Fixed-combination Drug Product and Single-component Dapagliflozin and Metformin Extended-release Tablets in Healthy Russian Subjects. *Clinical therapeutics*, 40(4):550–561.e3, Apr. 2018. ISSN 1879-114X 0149-2918. doi: 10.1016/j.clinthera.2018.02.006.

D. Kim, M. Choi, B. H. Jin, T. Hong, C. O. Kim, B. W. Yoo, and M. S. Park. Pharmacokinetic and pharmacodynamic drug-drug interactions between evogliptin and empagliflozin or dapagliflozin in healthy male volunteers. *Clinical and translational science*, 16(8):1469–1478, Aug. 2023a. ISSN 1752-8062 1752-8054. doi: 10.1111/cts.13566.

H. C. Kim, S. Lee, S. Sung, E. Kim, I.-J. Jang, and J.-Y. Chung. A Comparison of the Pharmacokinetics and Safety of Dapagliflozin Formate, an Ester Prodrug of Dapagliflozin, to Dapagliflozin Propanediol Monohydrate in Healthy Subjects. *Drug design, development and therapy*, 17:1203–1210, 2023b. ISSN 1177-8881. doi: 10.2147/DDDT.S404182.

B. Komoroski, N. Vachharajani, D. Boulton, D. Kornhauser, M. Geraldes, L. Li, and M. Pfister. Dapagliflozin, a novel SGLT2 inhibitor, induces dose-dependent glucosuria in healthy subjects. *Clinical pharmacology and therapeutics*, 85(5):520–526, May 2009. ISSN 1532-6535 0009-9236. doi: 10.1038/clpt.2008.251.

M. König. Sbmlsim: SBML simulation made easy. [object Object], Sept. 2021.

M. König. Sbmlutils: Python utilities for SBML. Zenodo, Aug. 2024.

M. König, A. Dräger, and H.-G. Holzhütter. CySBML: A Cytoscape plugin for SBML. *Bioinformatics*, 28(18):2402–2403, Sept. 2012. ISSN 1367-4811, 1367-4803. doi: 10.1093/bioinformatics/bts432.

F. LaCreta, S. C. Griffen, X. Liu, C. Smith, C. Hines, K. Volk, R. Tejwani, and D. W. Boulton. Bioequivalence and food effect of heat-stressed and non-heat-stressed dapagliflozin 2.5- and 10-mg tablets. *International journal of pharmaceutics*, 511(1):288–295, Sept. 2016. ISSN 1873-3476 0378-5173. doi: 10.1016/j.ijpharm.2016.07.017.

M. L. Neal, M. König, D. Nickerson, G. Mısırlı, R. Kalbasi, A. Dräger, K. Atalag, V. Chelliah, M. T. Cooling, D. L. Cook, S. Crook, M. de Alba, S. H. Friedman, A. Garny, J. H. Gennari, P. Gleeson, M. Golebiewski, M. Hucka, N. Juty, C. Myers, B. G. Olivier, H. M. Sauro, M. Scharm, J. L. Snoep, V. Touré, A. Wipat, O. Wolkenhauer, and D. Waltemath. Harmonizing semantic annotations for

computational models in biology. *Briefings in Bioinformatics*, 20(2):540–550, Mar. 2019. ISSN 1477-4054. doi: 10.1093/bib/bby087.

M. L. Neal, J. H. Gennari, D. Waltemath, D. P. Nickerson, and M. König. Open modeling and exchange (OMEX) metadata specification version 1.0. June 2020. doi: 10.18452/32800.

N. Nemitz, M. Elias, and M. König. Physiologically based pharmacokinetic/ pharmacodynamic (PBPK/PD) model of dapagliflozin. Zenodo, Dec. 2025.

M. Obermeier, M. Yao, A. Khanna, B. Koplowitz, M. Zhu, W. Li, B. Komoroski, S. Kasichayanula, L. Discenza, W. Washburn, W. Meng, B. A. Ellsworth, J. M. Whaley, and W. G. Humphreys. In vitro characterization and pharmacokinetics of dapagliflozin (BMS-512148), a potent sodium-glucose cotransporter type II inhibitor, in animals and humans. *Drug metabolism and disposition: the biological fate of chemicals*, 38(3):405–414, Mar. 2010. ISSN 1521-009X 0090-9556. doi: 10.1124/dmd.109.029165.

S. Sha, D. Polidori, K. Farrell, A. Ghosh, J. Natarajan, N. Vaccaro, J. Pinheiro, P. Rothenberg, and L. Plum-Mörschel. Pharmacodynamic differences between canagliflozin and dapagliflozin: Results of a randomized, double-blind, crossover study. *Diabetes, obesity & metabolism*, 17(2): 188–197, Feb. 2015. ISSN 1463-1326 1462-8902. doi: 10.1111/dom.12418.

P. A. Shah, P. S. Shrivastav, J. V. Shah, and A. George. Simultaneous quantitation of metformin and dapagliflozin in human plasma by LC-MS/MS: Application to a pharmacokinetic study. *Biomedical chromatography : BMC*, 33(4):e4453, Apr. 2019. ISSN 1099-0801 0269-3879. doi: 10.1002/bmc.4453.

L. P. Smith, M. Hucka, S. Hoops, A. Finney, M. Ginkel, C. J. Myers, I. Moraru, and W. Liebermeister. SBML Level 3 package: Hierarchical Model Composition, Version 1 Release 3. *Journal of Integrative Bioinformatics*, 12(2):268, Sept. 2015. ISSN 1613-4516. doi: 10.2390/biecoll-jib-2015-268.

E. T. Somogyi, J.-M. Bouteiller, J. A. Glazier, M. König, J. K. Medley, M. H. Swat, and H. M. Sauro. libRoadRunner: A high performance SBML simulation and analysis library. *Bioinformatics*, 31(20): 3315–3321, Oct. 2015. ISSN 1367-4811, 1367-4803. doi: 10.1093/bioinformatics/btv363.

A. B. van der Aart-van der Beek, A. M. A. Wessels, H. J. L. Heerspink, and D. J. Touw. Simple, fast and robust LC-MS/MS method for the simultaneous quantification of canagliflozin, dapagliflozin and empagliflozin in human plasma and urine. *Journal of chromatography. B, Analytical technologies in the biomedical and life sciences*, 1152:122257, Sept. 2020. ISSN 1873-376X 1570-0232. doi: 10.1016/j.jchromb.2020.122257.

H. Watada, M. Shiramoto, S. Ueda, W. Tang, M. Asano, F. Thorén, H. Kim, T. Yajima, D. W. Boulton, and E. Araki. Pharmacokinetics and pharmacodynamics of dapagliflozin in combination with insulin in Japanese patients with type 1 diabetes. *Diabetes, obesity & metabolism*, 21(4):876–882, Apr. 2019. ISSN 1463-1326 1462-8902. doi: 10.1111/dom.13593.

C. Welsh, J. Xu, L. Smith, M. König, K. Choi, and H. M. Sauro. libRoadRunner 2.0: A high performance SBML simulation and analysis library. *Bioinformatics*, 39(1):btac770, Jan. 2023. ISSN 1367-4811. doi: 10.1093/bioinformatics/btac770.

L. Yang, H. Li, H. Li, A. Bui, M. Chang, X. Liu, S. Kasichayanula, S. C. Griffen, F. P. Lacreta, and D. W. Boulton. Pharmacokinetic and pharmacodynamic properties of single- and multiple-dose of dapagliflozin, a selective inhibitor of SGLT2, in healthy Chinese subjects. *Clinical therapeutics*, 35(8):1211–1222.e2, Aug. 2013. ISSN 1879-114X 0149-2918. doi: 10.1016/j.clinthera.2013.06.017.